

Electronic Supplementary Information

Synthesis of DABCO-based Ionic liquid functionalized magnetic nanoparticles as a novel sorbent for determination of cephalosporins in milk samples by dispersive solid-phase extraction followed by ultra-performance liquid chromatography-tandem mass spectrometry

Hamed Sahebi, Elaheh Konoz * and Ali Ezabadi

^a: Department of Chemistry, Faculty of Science, Islamic Azad University Central Tehran Branch, Tehran, Iran.

corresponding author: Elaheh Konoz

Email: Konozelaheh@gmail.com

Tell/Fax: +982188074907

List of Contents

Supplementary Manuscript	3
Milk samples pre-treatment	3
Optimization of MS/MS detection and chromatographic separation	4
Thermal stability study of IL	6
XPS analysis	7
Screening significant parameters by fractional factorial design	8
Box-Behnken experimental design	9
Desirability function	10
The response surface plot.....	12
References.....	13
Supplementary Figures	14
Fig. S1. General chemical structure of CPL antibiotics.....	14
Fig. S2. FE-SEM image of a) Fe ₃ O ₄ NPs, b) Fe ₃ O ₄ @SiO ₂ NPs, c) Fe ₃ O ₄ @CPTMS NPs.....	15
Fig. S3. XPS spectra and High resolution XPS spectra of Fe ₃ O ₄ @[DABCO-DHP][Cl] NPs, a) C1s, b) N1s, C) Si2p, d) O1s.	16
Fig. S4. a) TGA profile of [DABCO-DHP][Cl], b) DSC of [DABCO-DHP][Cl].	17
Fig. S5. Effect of sorbent type.	18
Fig. S6. Pareto chart of CFQ.....	19
Fig. S7. 3D response surface plots for the ER% of CFM versus a) sorbent dosage and contact time, b) sorbent dosage and desorption time.....	20
Fig. S8. UPLC-MS/MS chromatograms of positive Sample2 after the D-μ-SPE procedure.....	21
Table S1. MS/MS parameters of the CPLs and IS.....	22
Table S2: Results of FFD.....	23
Table S3: ANOVA for the second-order regression models.	24
Table S4: The regression equations of responses for nine CPLs.....	27
Table S5. CC _μ (μg.kg ⁻¹), and CC _β (μg.kg ⁻¹) obtained for nine analytes in different milk samples.....	28
Table S6. Application of the proposed method to analysis of raw cow milk.	29

Supplementary Manuscript

Milk samples pre-treatment

As mentioned in the previous contents, milk samples have very complex matrices which contain large amounts of fats, carbohydrates, proteins and other components which may have a significant influence in the extraction efficiency ¹. Therefore, the precipitation of protein and fats is a critical step in the sample preparation procedures to the extraction of each analyte from a complex matrix such as milk. The use of an acidic aqueous solution of the zinc salt with MeCN is suggested for the pre-treatment of milk samples. This solution is proposed based on a hybrid solution which is used by the International Dairy Federation for the treatment of milk in the lactulose analysis ². Among the main advantages of this precipitation solution which could be referred to is the fact that this solution not only precipitates proteins and fats simultaneously but also remains very clear solution after the centrifugation. Here, due to maximizing the extraction efficiency of analytes and also reducing the final residuals, the ratio of the precipitation solution/MeCN/sample was evaluated and optimized. For 5.0 g of milk sample, the volumes from 1.0 to 10.0 mL for both precipitation solution and MeCN were studied. The optimized amounts for precipitation solution and MeCN were 2.5 and 3.0 mL, respectively.

Optimization of MS/MS detection and chromatographic separation

The parameters of the mass spectrometer were optimized for performing the best responses for the quantification of each analyte. The MRM transitions as well as the values of collision energy and cone voltage for each analyte were optimized by direct infusion of the individual standard solution of each CPL at $1.0 \mu\text{g}\cdot\text{mL}^{-1}$ (in UPW with 0.1% (V/V) acetic acid) into the mass spectrometer using ESI⁺ mode in order to obtain a maximum sensitivity. The infusion process was performed by the mentioned chromatography conditions in section “**UPLC-MS/MS Condition**”. The experiments of MS/MS were accomplished by fragmentation of the protonated molecule $[\text{M-H}]^+$ which was selected as the precursor ion. The transitions of two precursor-product ions were monitored for each compound. The product ion (Q) which had the most frequency was selected for the quantification, while the less sensitive transition (I) was used for confirmation of the identification (see selected Q and I ions in Table S1). The whole of the selected transitions had a desirable selectivity during the analysis. The experiments demonstrated that some of these transitions had not adequate sensitivity when dwell times for all of the transitions were set at 0.1 second; as a result, the dwell times of these transitions were set at 0.5, 0.20, or 0.25 in the scheduled MRM mode for the improvement of the sensitivity of the selected transitions. The optimized conditions of MRM for each analyte were summarized in Table S1.

Regarding the optimization of chromatographic conditions, aqueous standard solutions of CPLs were utilized when optimizing the separation. Firstly, a mobile phase containing UPW (solvent A) and MeOH (solvent B) both with formic acid (0.1% V/V) was utilized. Two chromatographic columns were investigated: BEH Shield C₁₈ (2.1 mm × 100 mm, 1.7 μm) and BEH Shield RP₁₈ (2.1 mm × 100 mm, 1.7 μm). The first one showed poor repeatability and selectivity regarding the most polar CPL molecules. Thus, BEH Shield RP₁₈ column was investigated, and results showed

that better selectivity and peak shapes were obtained for all the analytes while applying this column. Various organic solvents (solvent B) such as MeCN and MeOH were also investigated. The worse retention capacity was observed when using MeCN compared to MeOH. Thus, it was found that the CPLs' retention is higher on Embedded Phase when selecting MeOH as compared to using MeCN since this solvent provides hydrogen bond interactions with the Embedded polar groups in the stationary phase or the solutes available in the mobile phase. Therefore, MeOH was selected as solvent B. The acid should be used in the mobile phase so that the ionization in ESI⁺ mode is improved. Hence, different modifiers were investigated in aqueous and organic phases. The tested modifiers included acetic acid, formic acid, ammonium formate, and ammonium acetate. Significant differences were not observed in signals while using formic acid and ammonium formate. However, slightly higher signals were observed while ammonium acetate or/and acetic acid were used as the modifiers. Acetic acid provided better results in terms of sensitivity for all target analytes. The reason is that acetic acid is considered a weak acid modifier. Thus, the proton ions are more present, and the positive ionization is improved. However, signals showed no improvement in the ammonium acetate presence. Hence, the best choice was acetic acid, and in the mobile phase, it was selected as the modifier. Afterward, the acetic acid was tested at varying percentages in components A and B of the mobile phase. In the end, 0.1% (V/V) of acetic acid was selected in both elution solvents. Thus, the ultimate mobile phase was MeOH with 0.1% (V/V) acetic acid functioning as solvent B, and UPW with 0.1% (V/V) acetic acid serving as solvent A. The gradient optimization was done for getting the best separation and peak shape performance in the shorter period. For retarding the elution of the most polar compounds, it was required to start using with 100% Solvent A (aqueous solution). The optimum values were described in the section **“UPLC-MS/MS Condition”**.

Thermal stability study of IL

Thermal stability of synthesized IL was evaluated by TGA. The overlaps of TGA diagram and its first derivative (DTA) for [DABCO-DHP][Cl] is shown in Fig. S4a, and Fig. S4b indicated its differential scanning calorimetry (DSC) thermogram. In the first phase, the weight-loss in the range of temperature between ambient to 100 °C, was approximately 33% and the consistent DSC data in the range show that this change was related to an endothermic process. This loss of weight is most probably due to the removal of adsorbed water molecules. After initial water loss, the weight persists in being constant until achieving 220 °C, after which a sharp drop was observed in weight (30%); 235 °C was the first degradation temperature, as characterized by the DTA. This weight loss was also, according to DSC, an endothermic process and was most likely caused by the dequaternization of the ammonium cation. There was a gradual weight-loss of approximately 37%, immediately following this stage, which matches up to the second degradation temperature of 295 °C as indicated by the DTA. As shown in the DSC graph, similar to the previous step, it was an endothermic process as well.

XPS analysis

During modification processes, the chemical states can be verified by the use of the XPS technique. The XPS survey spectra of Fe_3O_4 , $\text{Fe}_3\text{O}_4@\text{SiO}_2$, $\text{Fe}_3\text{O}_4@\text{CPTMS}$, and $\text{Fe}_3\text{O}_4@[\text{DABCO-DHP}][\text{Cl}]$ samples are shown in Fig. S3, approving that all specimens have predominant peaks at 711.7 and 725.2 eV respectively due to Fe $2p_{3/2}$ and Fe $2p_{1/2}$ characteristics of iron oxide's core-level spectra that conform with the iron oxidation state in Fe_3O_4 (Fe^{2+} and Fe^{3+})^{3, 4}. For the $\text{Fe}_3\text{O}_4@\text{SiO}_2$ NPs, the XPS survey spectrum has peaks of Si2p, which confirmed that dense silica had been coated successfully. The XPS spectrum of $\text{Fe}_3\text{O}_4@\text{CPTMS}$ sample has detected chlorine element in comparison with $\text{Fe}_3\text{O}_4@\text{SiO}_2$, and for the $\text{Fe}_3\text{O}_4@[\text{DABCO-DHP}][\text{Cl}]$, the peak of chlorine element disappeared because of nucleophilic substitution reaction between nitrogen atoms and chlorine atoms resulting in the emergence of nitrogen element in the spectrum. The XPS analysis proves that the IL was successfully modified on the surface of magnetic NPs. Fig. S3 illustrates the prosperous graft of IL on the surface of the silica-coated Fe_3O_4 NPs in high-resolution XPS patterns. The high-resolution XPS spectra of C1s, N1s, Si2p, and O1s for the $\text{Fe}_3\text{O}_4@[\text{DABCO-DHP}][\text{Cl}]$ NPs are shown in Fig. S3a–d. Fig. S3a shows the C1s spectrum having an asymmetric peak structure attributed to the presence of variable carbons. The C1s peak can be deconvoluted into three chemically-shifted peak components at 284.6, 286.1, and 286.8 eV, allocated to C–C/C–H, C–N, and C–O, respectively. The peak situated at 286.1 eV is ascribed to C–N of quaternary amine⁵. The high-resolution N1s XPS spectrum (Fig. S3b) represents an intense peak at 402.1 eV assigning to positively charge N (N^+)⁶. The O1s and Si2p peaks have also demonstrated at 531.8 eV and 102.3 eV, respectively, ascribing the presence of Si–O linkage besides the oxygen functionalities on the silica surface coated on Fe_3O_4 NPs (Fig. S3c-d).

Screening significant parameters by fractional factorial design

A two-level fractional factorial design (FFD), (2_{IV}^{6-2}) with the design parameters (Table S2) was applied to screen the significant variables and to eliminate unnecessary variables. FFD includes 16 experimental runs, which was employed to screen significant factors influencing the ER of CPLs.

For economization of the necessary number of runs, every factor in a fractional design is typically set at two levels and responses are measured for only a portion of the probable combinations of levels. The low and high levels appointed by (-) and (+), respectively, were chosen according to previous experience and are denoted by real values, of which the outcomes are shown in Table S2. Based on the primary experimentations, six variables, viz. extraction time (A; 1-10 min), desorption time (B; 1-10 min), sample pH (C; 3-9), ionic strength (D; NaCl 1-10 %w/v), amount of sorbent (E; 10-100 mg) and temperature (F; 20-30 °C) were taken into account in screening.

Pareto chart displays the standardized effect of the FFD screening findings in the experiment. The bar lengths in the Pareto chart are proportionate to the extraction factors whereas the vertical line employs as the reference line representing a 95% confidence interval. Any effect arisen from a parameter that surpasses this reference line is taken significant in terms of extraction factors.

The obtained Pareto chart (Fig. S6) for CFQ (as an example) shows that the sample pH has the highest statistical effect on the extracting of CFQ. Besides, sorbent amount and the interaction effects between extraction time and desorption were detected to significant effect on extraction.

Box-Behnken experimental design

Conventional optimization methods namely one-variable-at-a time have an extensive application. They usually suffer from some disadvantages. These disadvantages are deficiency viz necessity, requiring a large number of experimental runs and chemical waste production, labor effort and being tedious and high cost. Moreover, these methods are incapable of differentiating between the significance of each variable, and as a result of that, the influences of interaction between variables are ignored, and the correct optimum level cannot be achieved. To overcome these impediments, multivariate optimization is an appropriate and valid statistical method capable of eliminating the restrictions of traditional optimization ⁷. Response surface methodology is a dominant statistical-based strategy to evaluate the effects of different factors simultaneously which enables the optimum conditions for providing the desirable response ^{8, 9}. The Box–Behnken design-based response surface methodology enables us to distinguish discrete variables and their interactions on target response empirically polynomial function with minimum time and cost. Thus, appreciated info was achieved for a predetermined procedure using the methodologies of the experimental strategy. Responses are considered as dependent variables, and factors are independent variables ¹⁰.

The fitting and analysis of the data resulting from the experiment design comply with the second-order polynomial model and the general form of which for response surface analysis will be described in the following ¹¹.

$$Y = \beta_0 + \sum_{i=1}^k \beta_i x_i + \sum_{i=1}^k \beta_{ii} x_i^2 + \sum_{i=1}^{k-1} \sum_{j=2}^k \beta_{ij} x_i x_j \quad (1)$$

Where Y is the predicted response, X_i and X_j are the independent variables that, these are the experimental factors, and β_0 , β_i , β_{ii} , and β_{ij} are the regression coefficients for the intercept, linear, quadratic, and interaction terms, respectively.

The analysis of variance statistical test is used for the analysis of variances and analyzes significance factors and their mutual interactions and on other factors. By the use of the response surface methodology, the validated model is then designed in three dimensions followed by interpretation for finding optimum condition for the procedure.

Desirability function

To obtain the global optimal conditions based on Derringer's desirability function, desirability function is a common and routine technique since it differentiates and reaches an input variable, makes a function for each individual response and in the end determines a global function that shall be maximized accompanying variety of optimum amount of affective variables, taking into account their interaction ¹².

Qualitative and quantitative information can be obtained by desirability functions since it metamorphoses various responses and relates team to measurement. The response (Y) is converted into desirability function (df_i) in the range of 0 to 1 (where values near zero and one recommend non-desirable and very desirable), all of which can be calculated and formulated according to the following equation.

$$df_i = \left(\frac{Y - \alpha}{\beta - \alpha}\right)^{wi}, \alpha \leq Y \leq \beta$$

$$df_i = 1, Y > \beta \tag{2}$$

$$df_i = 0, Y < \alpha$$

i and w_i are the weight and α , and β are the minimum and maximum gained values of the response in equation 2. The overall desirability function is mixed with each individual desirability score for the predicted values by computing their geometric mean of different df_i values.

$$DF = [df_1^{v_1} \times df_2^{v_2} \dots \times df_n^{v_n}]^{\left(\frac{1}{n}\right)}, 0 \leq v_i \leq 1 (i = 1, 2, \dots, n) \quad (3)$$

$$\sum_{i=1}^n v_i = 1$$

Where df_i indicates the desirability of the response Y_i ($i = 1, 2, 3, \dots, n$) and v_i represents the desirability of each response on the dependent variables ¹³.

The response surface plot

The effects of three parameters on ER percentages of nine CPLs (taken CFM as an example) are showed in Fig. S7. Factors significantly influenced the ER included the linear effect of sorbent dosage, contact time and desorption time (p -value < 0.0001), the interaction effect between the sorbent dosage and contact time (p -value < 0.047), and the one between the sorbent dosage and desorption time (p -value < 0.014), as well as all the quadratic effects.

The response surface plot (Fig. S7a) for the simultaneous effect of sorbent dosage and contact time at constant desorption time (3 min) revealed that at any fixed extraction time levels, the ER percentage increases with increasing sorbent dose. It is evident from Fig. S6a that the highest contact time is not required to gain the maximum ER. As it is observed in the obtained results, a relative response is enhanced by raising the contact time, and the maximum ER was achieved at an extraction time of 3.5 minutes. Achievement of such a short time is assigned to the acceleration of the mass transfer by analytes, which cause enhancement of the extraction kinetic¹⁴. Above 3.5 min, the percentage ER decreases due to the desorption of some analytes from the absorbent surface. On the other hands, increase in the sorbent mass at higher sonication time likely results in aggregation of the sorbent.

The interaction effect of sorbent quantity and desorption time (Fig. S6b) leads to the conclusion that they significantly affect the ER. At the range of 20 mg to 70 mg sorbent dose, the ER was enhanced, with a sharp slope driven by increasing desorption time from all sorbent quantities,

while an increase in the desorption time levels did not have a positive effect on ER from the 75 mg quantity to the 80 mg. The ER decreased by allocating a higher amount of the Fe₃O₄@-[DABCO-DHP][Cl] NPs, more than 75 mg, elaborating that additional quantity of sorbent was not helpful with small volumes of the extraction solvent ¹⁵.

References

1. D. Moreno-González, A. M. Hamed, A. M. García-Campaña and L. Gámiz-Gracia, *Talanta*, 2017, **171**, 74-80.
2. I. O. f. S. I. D. Federation, *Journal*, 2007.
3. X. Teng, D. Black, N. J. Watkins, Y. Gao and H. Yang, *Nano Letters*, 2003, **3**, 261-264.
4. R. Liu, Y. Zhao, R. Huang, Y. Zhao and H. Zhou, *European Journal of Inorganic Chemistry*, 2010, **2010**, 4499-4505.
5. L. Bekalé, S. Barazzouk and S. Hotchandani, *Journal of Materials Chemistry*, 2012, **22**, 2943-2951.
6. A. Maetz, L. Delmotte, G. Moussa, J. Dentzer, S. Knopf and C. M. Ghimbeu, *Green Chemistry*, 2017, **19**, 2266-2274.
7. A. R. Bagheri, M. Arabi, M. Ghaedi, A. Ostovan, X. Wang, J. Li and L. Chen, *Talanta*, 2019, **195**, 390-400.
8. B. H. Hameed, I. A. W. Tan and A. L. Ahmad, *Journal of Hazardous Materials*, 2008, **158**, 324-332.
9. J. N. Sahu, J. Acharya and B. C. Meikap, *Journal of Hazardous Materials*, 2009, **172**, 818-825.
10. T. U. Nwabueze, *International Journal of Food Science & Technology*, 2010, **45**, 1768-1776.
11. S. L. C. Ferreira, R. E. Bruns, H. S. Ferreira, G. D. Matos, J. M. David, G. C. Brandão, E. G. P. da Silva, L. A. Portugal, P. S. dos Reis, A. S. Souza and W. N. L. dos Santos, *Analytica Chimica Acta*, 2007, **597**, 179-186.
12. A. Malenović, Y. Dotsikas, M. Mašković, B. Jančić–Stojanović, D. Ivanović and M. Medenica, *Microchemical Journal*, 2011, **99**, 454-460.
13. M. Roosta, M. Ghaedi and M. Mohammadi, *Powder Technology*, 2014, **267**, 134-144.
14. A. Ostovan, H. Asadollahzadeh and M. Ghaedi, *Ultrasonics Sonochemistry*, 2018, **43**, 52-60.
15. Q. Wen, Y. Wang, K. Xu, N. Li, H. Zhang, Q. Yang and Y. Zhou, *Talanta*, 2016, **160**, 481-488.

Supplementary Figures

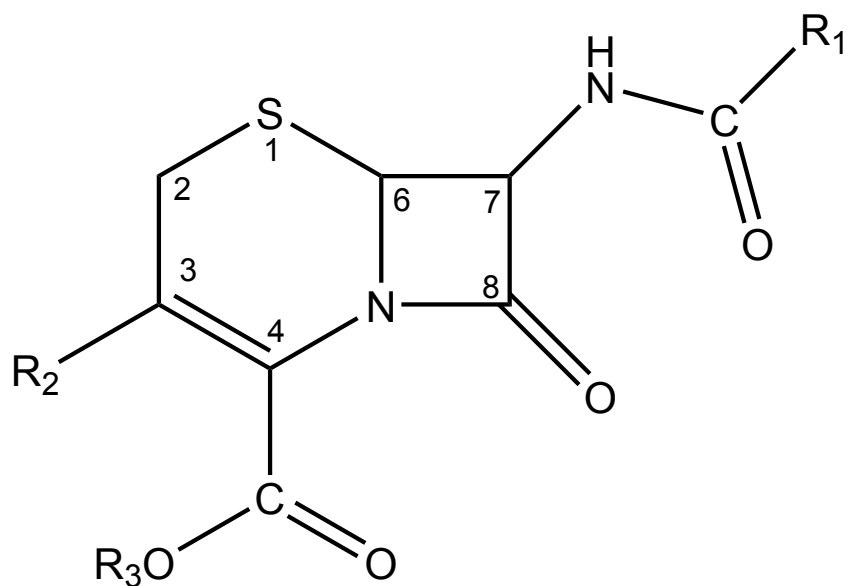


Fig. S1. General chemical structure of CPL antibiotics.

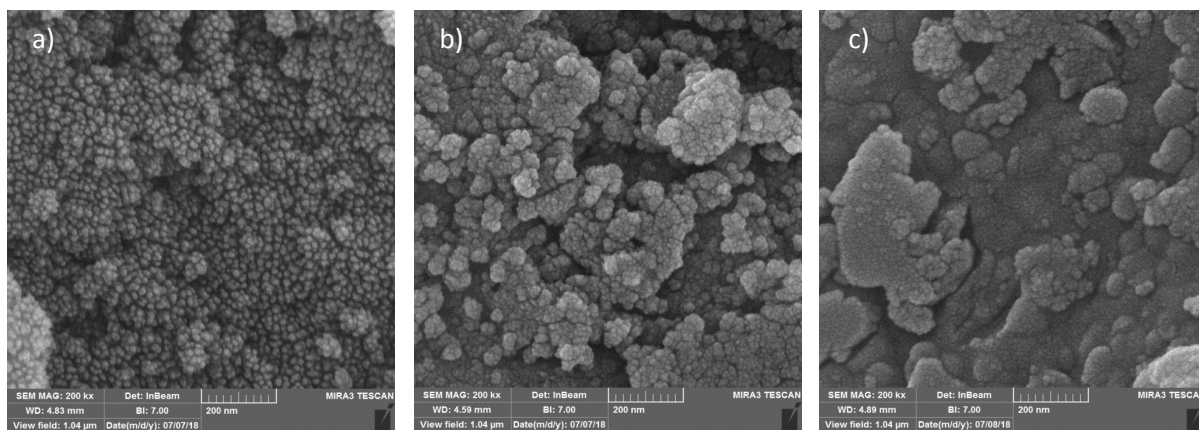


Fig. S2. FE-SEM image of **a)** Fe₃O₄ NPs, **b)** Fe₃O₄@SiO₂ NPs, **c)** Fe₃O₄@CPTMS NPs.

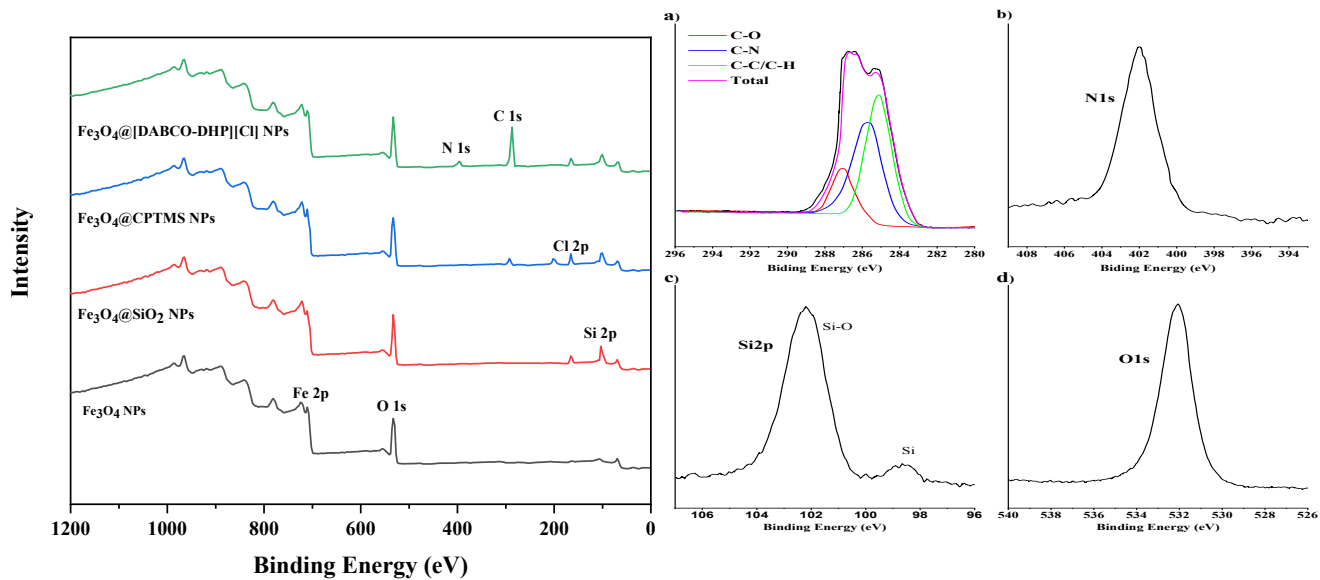


Fig. S3. XPS spectra and High resolution XPS spectra of Fe₃O₄@[DABCO-DHP][Cl] NPs, a) C 1s, b) N 1s, c) Si 2p, d) O 1s.

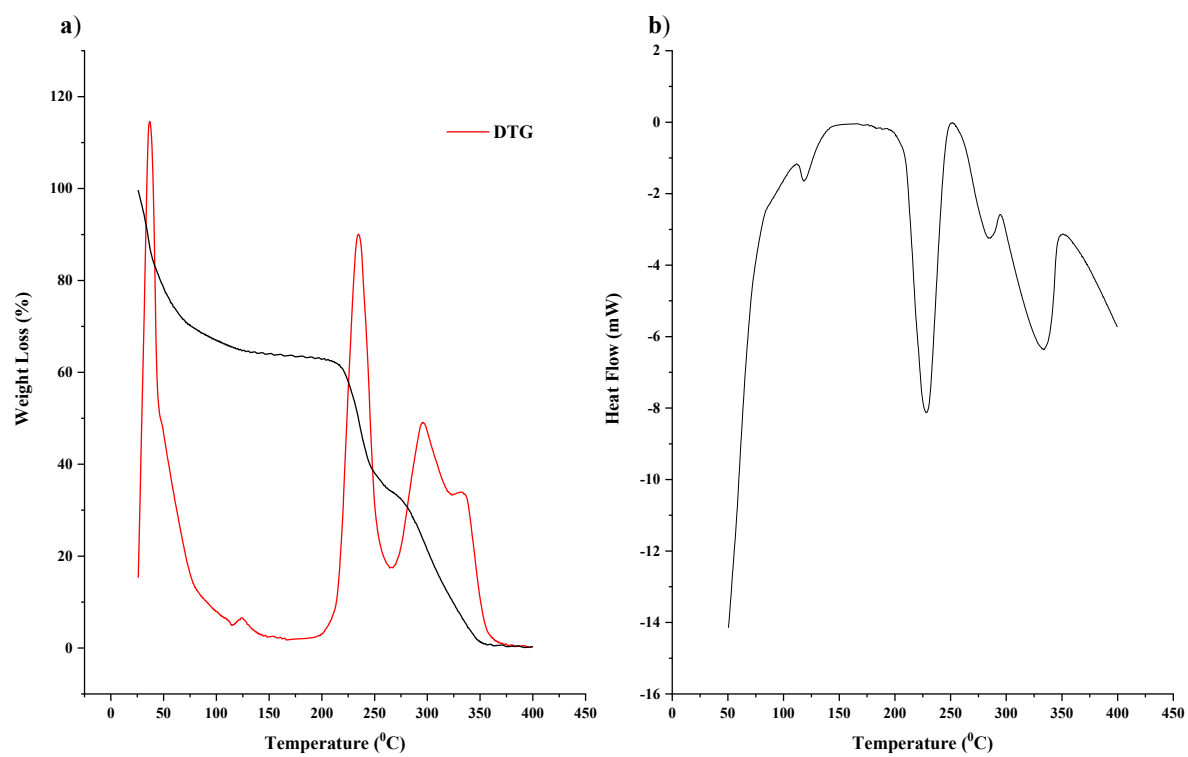


Fig. S4. a) TGA profile of [DABCO-DHP][Cl], **b)** DSC of [DABCO-DHP][Cl].

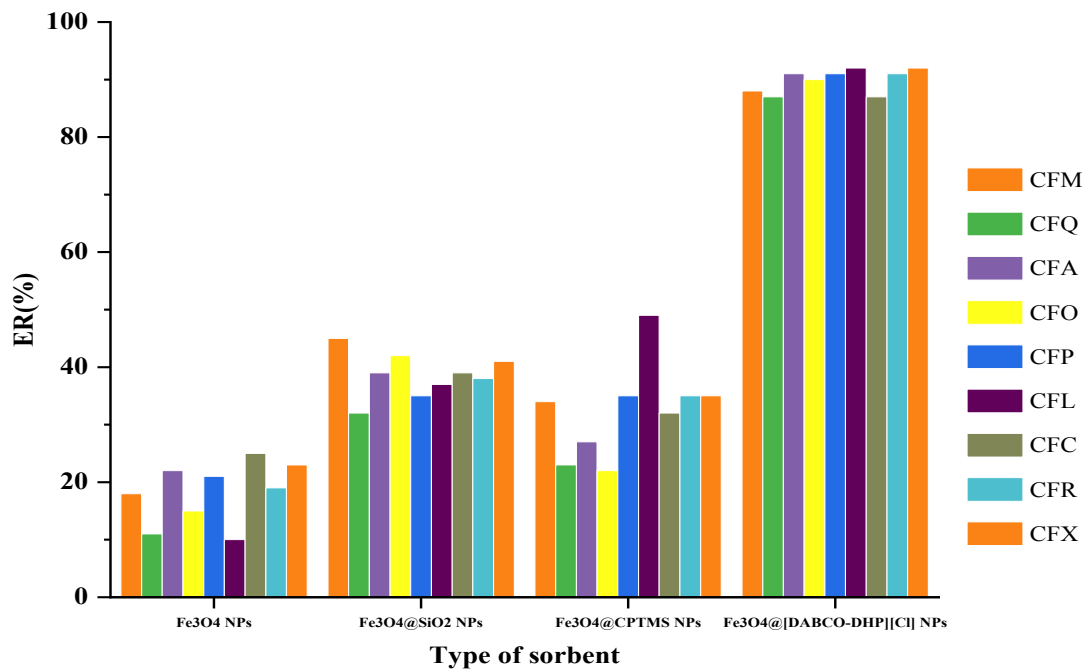


Fig. S5. Effect of sorbent type.

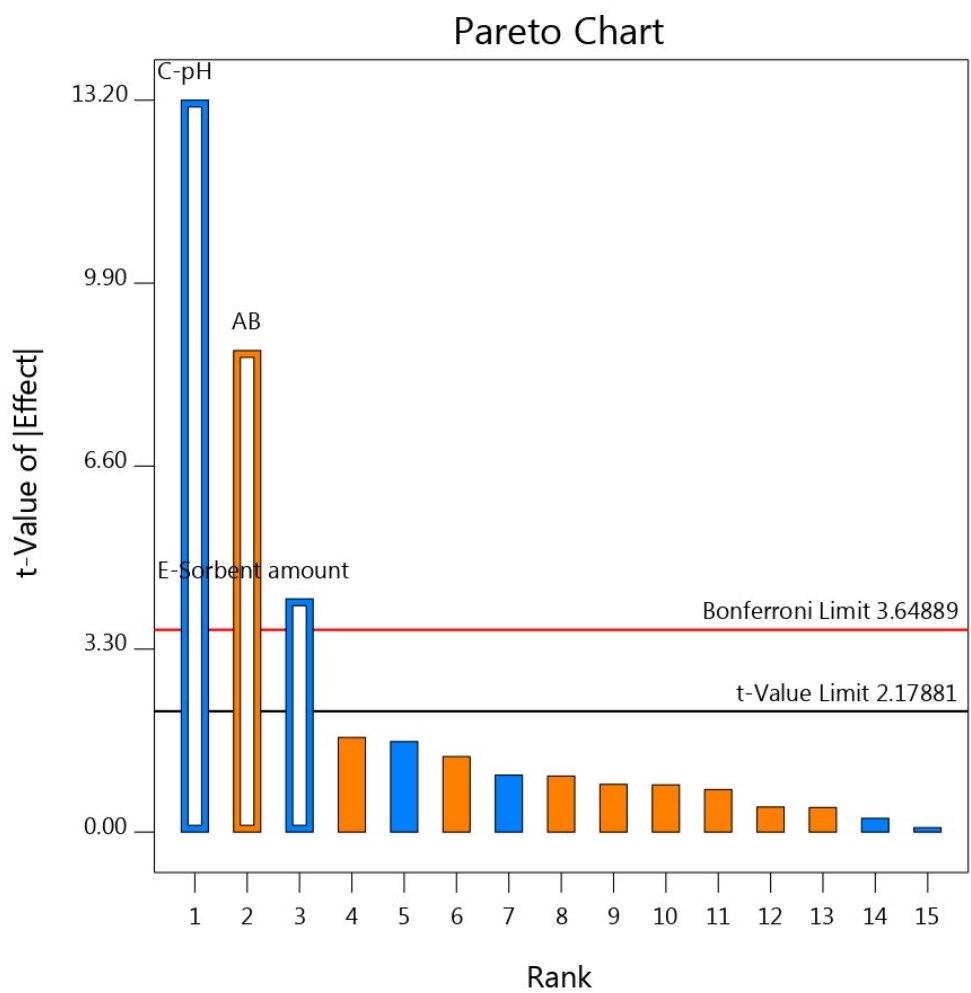


Fig. S6. Pareto chart of CFQ.

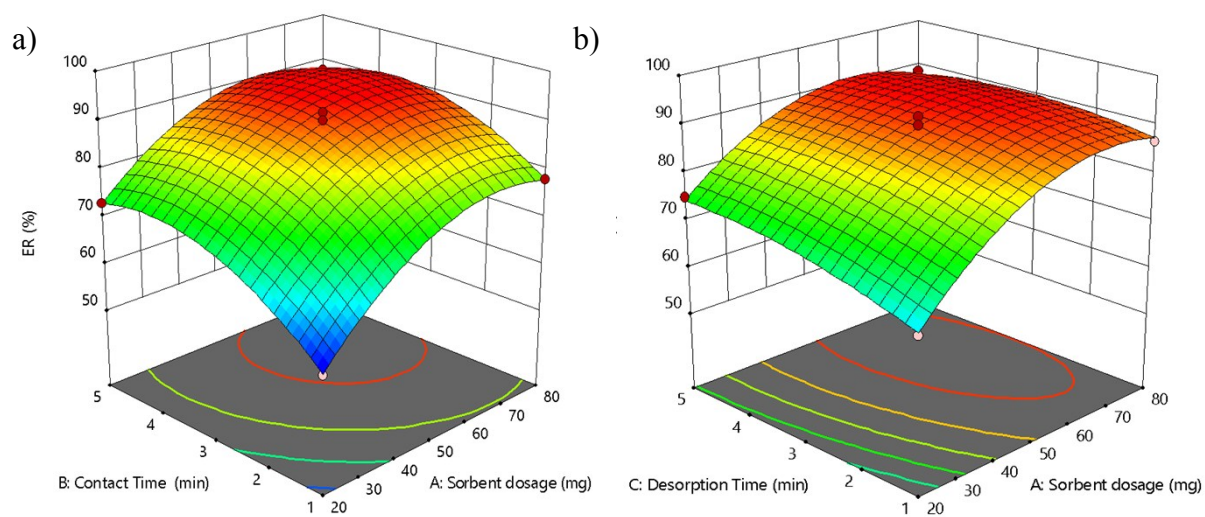


Fig. S7. 3D response surface plots for the ER% of CFM versus **a)** sorbent dosage and contact time, **b)** sorbent dosage and desorption time.

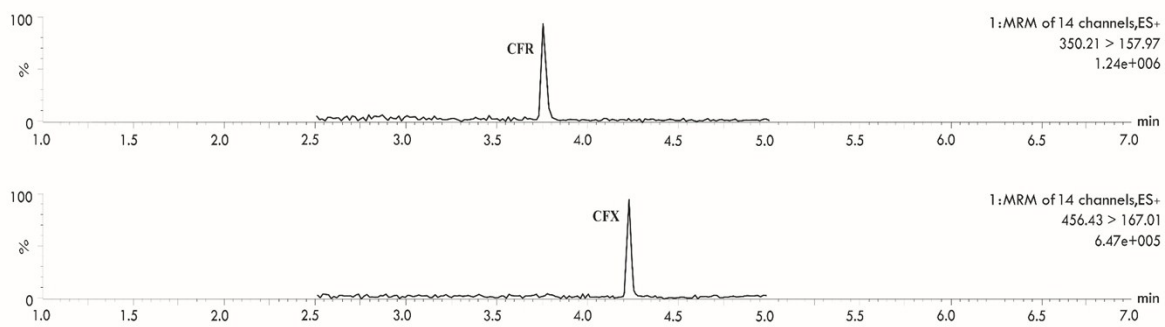


Fig. S8. UPLC-MS/MS chromatograms of positive SampleR2 after the D- μ -SPE procedure.

Table S1. MS/MS parameters of the CPLs and IS.

Analyte	Precursor ion (m/z)	Product ion (m/z)	Dwell time (s)	Collision energy (eV)	Cone voltage (V)
CFM	459.29	151.97 (Q)	0.1	18	18
		337.1 (I)	0.2	10	
CFQ	529.38	134.13 (Q)	0.1	14	24
		396.12 (I)	0.25	12	
CFA	455.25	156.00 (I)	0.25	16	20
		323.15(Q)	0.25	10	
CFO	646.45	143.05 (Q)	0.25	32	22
		290.13 (I)	0.25	24	
CFP	424.44	152.04 (Q)	0.1	20	24
		292.24 (I)	0.1	14	
CFL	348.23	158.02 (I)	0.1	8	16
		174.10 (Q)	0.1	16	
CFC	362.17	178.01 (I)	0.1	14	24
		258.06 (Q)	0.1	12	
CFR	350.21	157.97 (I)	0.1	12	18
		176.06 (Q)	0.1	18	
CFX	456.43	167.01 (I)	0.1	20	22
		396.16 (Q)	0.2	10	
CFI-D3	527.29	125.02 (I)	0.25	30	54

Q: Ion for quantification, I: Ion for identification.

Table S2:
Results of FFD.

Run	Factor ^a						Responses (ER%)								
	A	B	C	D	E	F	CFM	CFQ	CFA	CFO	CFP	CFL	CFC	CFR	CFX
1	1	-1	-1	-1	1	-1	44.8	46.3	43.8	47.5	40.5	40	42.3	41.2	39.3
2	-1	1	1	-1	-1	-1	12.1	13.2	13.5	12.4	14.3	12.6	14.3	17.6	19.6
3	1	1	1	1	1	1	30.6	32.4	28.5	29.7	31.3	30.7	29.4	33.4	27.6
4	-1	1	1	1	-1	1	17.1	19.2	19.2	16.8	20.2	18.6	15.7	21.3	16.7
5	-1	-1	1	-1	1	1	23.8	25.3	27.6	31.2	26.3	25.2	27.6	25.4	26.4
6	-1	-1	-1	-1	-1	-1	67.1	64.2	57.3	63.5	63.4	62.3	65.2	63.3	62.2
7	1	1	-1	1	-1	-1	82.1	80.6	80.4	79.8	81.6	83.4	80.4	81.1	78.9
8	1	1	1	-1	1	-1	23	24.5	26.2	25.6	26.4	27.3	25.7	27.6	29.3
9	1	-1	1	1	-1	-1	9.8	13.4	14.2	10.7	12.3	12.3	11.2	13.6	12.4
10	-1	-1	1	1	1	-1	21.4	23.4	22.1	24.6	23.7	25.7	23.3	23.5	23.5
11	-1	1	-1	-1	1	1	30.2	32	33.5	33.4	34.8	31.3	31.9	34.3	31.3
12	1	-1	1	-1	-1	1	9.4	11.6	17.4	14.5	11.2	10.5	9.5	9.5	13.5
13	1	1	-1	-1	-1	1	76.3	73.3	78.5	75.6	72.6	74.2	75.4	71.6	72.6
14	-1	1	-1	1	1	-1	33.7	34.6	30.2	32.1	31.8	34.6	30.6	36.5	31.3
15	-1	-1	-1	1	-1	1	75.3	74.8	78.4	74.3	75.6	76.2	77.2	70.6	68.3
16	1	-1	-1	1	1	1	40.9	41.3	46.2	43.7	42.2	43.4	41.2	38.6	40.2

a: A: Contact Time (min), B: Desorption Time (min), C: pH, D: NaCl solution concentration (%). E: Sorbent amount (mg), F: Temperature (°C).

Table S3: ANOVA for the second-order regression models.

Analyte Source ^a	CFM				CFQ				CFA			
	Sum of Squares	Mean Square	F-value	p-value	Sum of Squares	Mean Square	F-value	p-value	Sum of Squares	Mean Square	F-value	p-value
Model	1612.45	179.16	118.73	< 0.0001	1484.38	164.93	58.99	< 0.0001	1548.44	172.05	52.7	< 0.0001
A	626.58	626.58	415.23	< 0.0001	586.53	586.53	209.79	< 0.0001	574.61	574.61	176	< 0.0001
B	322.58	322.58	213.77	< 0.0001	320.05	320.05	114.47	< 0.0001	280.85	280.85	86.02	< 0.0001
C	42.32	42.32	28.05	0.0011	24.15	24.15	8.64	0.0217	38.72	38.72	11.86	0.0108
AB	8.7	8.7	5.77	0.0474	7.56	7.56	2.7	0.144	10.56	10.56	3.24	0.1151
AC	15.6	15.6	10.34	0.0147	16	16	5.72	0.048	28.62	28.62	8.77	0.0211
BC	5.06	5.06	3.35	0.1097	5.06	5.06	1.81	0.2204	0.3025	0.3025	0.0927	0.7697
A ²	305.82	305.82	202.67	< 0.0001	277.28	277.28	99.18	< 0.0001	338.97	338.97	103.83	< 0.0001
B ²	216.61	216.61	143.55	< 0.0001	180.09	180.09	64.42	< 0.0001	216.61	216.61	66.35	< 0.0001
C ²	20.8	20.8	13.78	0.0075	23.55	23.55	8.42	0.0229	12.49	12.49	3.83	0.0913
Residual	10.56	1.51			19.57	2.8			22.85	3.26		
Lack of Fit	3.22	1.07	0.5834	0.6569	10.02	3.34	1.4	0.3653	6.71	2.24	0.5536	0.6726
Pure Error	7.35	1.84			9.55	2.39			16.15	4.04		
Cor Total	1623.02				1503.96				1571.3			
R ²		0.9935				0.987				0.9855		
		0.9851				0.9703				0.9668		
Predicted R ²		0.9612				0.8835				0.9157		
Adeq Precision		34.7609				24.3292				23.2142		

a: A=Sorbent dosage (mg), B=Contact time (min), C=Desorption time (min).

Continued Table S3.

Analyte Source	CFO				CFP				CFL			
	Sum of Squares	Mean Square	F-value	p-value	Sum of Squares	Mean Square F-value	p-value	Sum of Squares	Mean Square	F-value	p-value	
Model	1686.91	187.43	151.68	< 0.0001	1669.93	185.55	76.76	< 0.0001	1583.53	175.95	97.91	< 0.0001
A	633.68	633.68	512.8	< 0.0001	447	447	184.93	< 0.0001	596.85	596.85	332.12	< 0.0001
B	330.24	330.24	267.25	< 0.0001	136.95	136.95	56.66	0.0001	356.45	356.45	198.35	< 0.0001
C	48.02	48.02	38.86	0.0004	81.28	81.28	33.63	0.0007	40.95	40.95	22.79	0.002
AB	2.4	2.4	1.94	0.2059	157.5	157.5	65.16	< 0.0001	16.81	16.81	9.35	0.0184
AC	23.52	23.52	19.04	0.0033	6.5	6.5	2.69	0.145	2.4	2.4	1.34	0.2855
BC	7.56	7.56	6.12	0.0426	13.69	13.69	5.66	0.0489	5.29	5.29	2.94	0.1299
A ²	336.33	336.33	272.18	< 0.0001	430.37	430.37	178.04	< 0.0001	250.13	250.13	139.19	< 0.0001
B ²	242.4	242.4	196.16	< 0.0001	351.36	351.36	145.36	< 0.0001	248.51	248.51	138.29	< 0.0001
C ²	13.45	13.45	10.89	0.0131	13.12	13.12	5.43	0.0527	19.6	19.6	10.91	0.0131
Residual	8.65	1.24			16.92	2.42			12.58	1.8		
Lack of Fit	2.73	0.91	0.6149	0.6407	8.37	2.79	1.31	0.3882	5.41	1.8	1.01	0.4771
Pure Error	5.92	1.48			8.55	2.14			7.17	1.79		
Cor Total	1695.56				1686.85				1596.1			
R ²		0.9949				0.99				0.9921		
Adjusted R ²		0.9883				0.9771				0.982		
Predicted R ²		0.9688				0.9127				0.9388		
Adeq Precision		39.2926				32.6539				32.1085		

Continued Table S3.

Analyte Source	CFC				CFR				CFX			
	Sum of Squares	Mean Square	F-value	p-value	Sum of Squares	Mean Square	F-value	p-value	Sum of Squares	Mean Square	F-value	p-value
Model	1678.16	186.46	49.05	< 0.0001	1595.39	177.27	122.44	< 0.0001	664.3	664.3	213.65	< 0.0001
A	539.56	539.56	141.94	< 0.0001	612.5	612.5	423.06	< 0.0001	338	338	108.7	< 0.0001
B	363.15	363.15	95.53	< 0.0001	311.25	311.25	214.98	< 0.0001	18.91	18.91	6.08	0.0431
C	63.85	63.85	16.8	0.0046	41.86	41.86	28.91	0.001	0.0625	0.0625	0.0201	0.8913
AB	18.92	18.92	4.98	0.0609	6.76	6.76	4.67	0.0675	18.49	18.49	5.95	0.0449
AC	33.64	33.64	8.85	0.0207	10.89	10.89	7.52	0.0288	27.56	27.56	8.86	0.0206
BC	6.25	6.25	1.64	0.2406	6.5	6.5	4.49	0.0718	234.32	234.32	75.36	< 0.0001
A ²	295.86	295.86	77.83	< 0.0001	306.54	306.54	211.73	< 0.0001	179.82	179.82	57.83	0.0001
B ²	255.02	255.02	67.09	< 0.0001	227.93	227.93	157.43	< 0.0001	26.53	26.53	8.53	0.0223
C ²	43.32	43.32	11.4	0.0118	21.46	21.46	14.82	0.0063	21.77	3.11		
Residual	26.61	3.8			10.13	1.45			12.26	4.09	1.72	0.3005
Lack of Fit	12.2	4.07	1.13	0.4375	1.4	0.4675	0.2142	0.882	9.51	2.38		
Pure Error	14.41	3.6			8.73	2.18			1571.82			
Cor Total	1704.77				1605.52							
R ²		0.9844				0.9937				0.9862		
Adjusted R ²		0.9643				0.9856				0.9683		
Predicted R ²		0.8723				0.9775				0.8658		
Adeq Precision		22.2622				35.0683				23.1807		

Table S4: The regression equations of responses for nine CPLs.

Analyte	Equation ^a
CFM	$Y_1 = +89.62 + 8.85A + 6.35B + 2.3C - 1.475AB - 1.975AC + 1.125BC - 8.5225A^2 - 7.1725B^2 - 2.2225C^2$
CFQ	$Y_2 = +90.28 + 8.5625A + 6.325B + 1.7375C - 1.375AB - 2AC + 1.125BC - 8.115A^2 - 6.54B^2 - 2.365C^2$
CFA	$Y_3 = +90.82 + 8.475A + 5.925B + 2.2C - 1.625AB - 2.675AC + 0.275BC - 8.9725A^2 - 7.1725B^2 - 1.7225C^2$
CFO	$Y_4 = +88.5 + 8.9A + 6.425B + 2.45C - 0.77AB - 2.425AC + 1.375BC - 8.9375A^2 - 7.5875B^2 - 1.7875C^2$
CFP	$Y_5 = +86.22 + 7.475A + 4.1375B + 3.1875C - 6.275AB - 1.275AC + 1.85BC - 10.11A^2 - 9.135B^2 + 1.765C^2$
CFL	$Y_6 = +87.34 + 8.6375A + 6.675B + 2.2625C - 2.05AB - 0.775AC + 1.15BC - 7.7075A^2 - 7.6825B^2 - 2.1575C^2$
CFC	$Y_7 = +87.44 + 8.2125A + 6.7375B + 2.825C - 2.175AB - 2.9AC + 1.25BC - 8.3825A^2 - 7.7825B^2 - 3.2075C^2$
CFR	$Y_8 = +90.34 + 8.75A + 6.2375B + 2.2875C - 1.3AB - 1.65AC + 1.275BC - 8.5325A^2 - 7.3575B^2 - 2.2575C^2$
CFX	$Y_9 = +90.92 + 9.1125A + 6.5B + 1.5375C - 0.125AB - 2.15AC + 2.625BC - 7.46A^2 - 6.535B^2 - 2.51C^2$

a: Y_{1-9} = ERs of CPLs (%), A=Sorbent dosage (mg), B=Contact time (min), C=Desorption time (min).

Table S5. CC μ ($\mu\text{g.kg}^{-1}$), and CC β ($\mu\text{g.kg}^{-1}$) obtained for nine analytes in different milk samples.

Analyte	MRL	Whole cow milk		Skimmed cow milk		Whole goat milk		Whole sheep milk		Cow raw milk	
		CC α	CC β	CC α	CC β	CC α	CC β	CC α	CC β	CC α	CC β
CFM	20	22	25	23	26	23	26	22	25	24	28
CFQ	20	23	26	22	25	22	25	23	26	24	28
CFA	50	53	59	54	60	54	60	55	61	56	62
CFO	50	54	60	55	61	55	61	54	60	57	62
CFP	60	66	75	66	76	67	77	67	77	68	79
CFL	100	112	126	113	127	112	126	113	128	128	133
CFC	125	138	154	139	153	139	153	139	153	141	158
CFR	/	0.1	0.14	0.11	0.16	0.11	0.15	0.12	0.17	0.22	0.35
CFX	/	0.12	0.16	0.112	0.116	0.13	0.18	0.13	0.17	0.33	0.48

Table S6. Application of the proposed method to analysis of raw cow milk.

Sample	CPL(s) found	Concentration ^a ($\mu\text{g}\cdot\text{kg}^{-1}$)	RSD (%)
R1	CFL	18	6.4
R2	CFX	29	5.9
	CFR	22	5.1
R3	CFL	31	5.9
R4	CFL	16	5.2
	CFR	9	5.7
R5	CFL	25	5.2
R6	CFX	14	5.6

a: Mean of five determinations.